14TH EUROPEAN CONFERENCE ON COMPOSITE MATERIALS
7-10 June 2010, Budapest, Hungary
Paper ID: 698-ECCM14

A 2.5 Simulation of the Resin Infusion Process, Addressing Complex Reinforcement Compaction Response

B. Verleye[1,*], P.A. Kelly[2], S. Bickerton[1]

[1] Centre for Advanced Composite Materials, Department of Mechanical Engineering, The University of Auckland, Private Bag 92019, Auckland, New Zealand
[2] Centre for Advanced Composite Materials, Department Engineering Science, The University of Auckland, Private Bag 92019, Auckland, New Zealand
*bver018@esc.auckland.ac.nz

Abstract

The simulation of composite manufacturing processes is a great aid to obtaining efficient production and high quality parts. The mould and process design must allow for fast filling times as well as dry-spot free parts. In previous work we presented our software SimLCM for the simulation of force and velocity controlled Resin Transfer Moulding (RTM) and Compression RTM. These are two examples of the general Liquid Composite Moulding (LCM) group of processes. Another recently popular subclass is Resin Infusion (RI), also know as Vacuum Assisted RTM. The simulation of RI adds an extra difficulty to the simulation process, as the height of the preform will change locally because of the filling. In contrast to CRTM, this change of height is not imposed, and thus not known beforehand. This paper describes the extension of SimLCM to the simulation of RI processes. The results of the simulations are compared with results from other programs that use different techniques, and also with experimentally obtained data found in literature. The comparison between simulation and experiment is found to be excellent.

1. Introduction

Two widely used composite production techniques are Resin Transfer Moulding (RTM) and Compression Resin Transfer Moulding (CRTM). They both involve the placement of a textile reinforcement in a two-sided solid mould, closure of the mould and resin injection. After the preparation, the mould can be closed with a constant velocity (velocity controlled) or with an imposed clamping force (force controlled). When RTM is used, the mould is closed to its final thickness before resin is injected. With CRTM, the mould is only partially closed before resin injection; after injection, the mould is closed to the final thickness, driving the resin further through the preform with compression driven flow. In addition, this compression stage can be velocity or force controlled. Finally, the part is cured, and released from the mould.

Both RTM and CRTM use solid moulds that do not change shape during the whole process. Another popular technique uses a flexible plastic bag as the upper mould. Under the bag vacuum is pulled, vent lines being connected to a vacuum pump. Away from the pump, an inlet is provided with resin under atmospheric pressure. The pressure difference between the atmospheric pressure and the vacuum pulled at the vent drives the resin through the textile reinforcement. The total pressure on the bag is the atmospheric pressure, and this must equal the sum of the resin fluid pressure and the pressure taken up by the reinforcement. This implies that as the fluid flows through the laminate, the fluid pressure will rise, and the reinforcement will unload, increasing local laminate thickness.

A composite manufacturer will be interested in choosing the most cost effective production process and required tooling equipment to manufacture the desired composite product. Hereby a trade off has to be made between the required clamping force, the process time and cost of moulds and other supporting equipment. These considerations help in designing the appropriate manufacturing tools cost effectively. Whilst a wide variety of RTM [1,14,15,18,19,20] and CRTM [2,3,4,7,16,17] filling simulations have been described in the literature, in the vast majority of cases these codes have been used to consider resin flow only. However, the total stress acting on a mould surface is the sum of the internally generated fluid pressure and the preform compaction stress. Thus, not only the characteristics of the fluid, but also the compaction response of the preform has an important influence on the total clamping force. Fibrous materials are most often assumed to behave as purely elastic when compacted and then held at a constant thickness. More elaborate models allow for viscoelastic effects, which yield more accurate predictions.

The simulation of Resin Infusion (RI) processes has been addressed in the literature, however, the simulations are usually in 1D or use simplified models for the compaction behaviour. In the RI case, the compaction response of the reinforcement is crucial as this will influence the filling time to a large extent, and also the eventual thickness of the produced part.

SimLCM is a finite element based code developed at the University of Auckland to address the Liquid Composite Moulding (LCM) family of manufacturing processes. This paper describes the extension of SimLCM to include the simulation of RI. First, the paper explains the simulation of CRTM and the viscoelastic reinforcement compaction model employed. This will illustrate the importance of allowing for viscoelastic effects. Then, the extension towards RI is explained. The results of RI simulations are compared with results from other simulations and experiments found in the literature. Finally, the further steps towards a more accurate simulation, in particular concerning the post-processing stage, are addressed.

2. Modelling of flow and fabric stress

2.1. Equations of flow

The fluid flow inside the mould and through the preform is generally computed by solving Darcy's law combined with conservation of fluid and fibre mass,

	Ten layers 280g glass Twill [13]	Textile as used in [8]
Compressibility wet h (m)	$h=0.0029186(p_{atm}-p)^{-0.0559}$	$h=0.02 \times \exp(-((p_{atm}-p)/5500)^{(1/6)})$
Compressibility dry h (m)	$h=0.0058786(p_{atm}-p)^{-0.1013}$	$h=0.02 \times \exp(-((p_{atm}-p)/125000)^{(1/5)})$
Uncompressed thickness (m)	h=0.00287	h=0.02
Permeability (m^2)	$K=8.827 \times 10^{-7} h^{1.8375}$	$K=2e^{-11}((1-V_f)^3/V_f^2)$
Resin viscosity (Pa s)	0.346	0.1
Used vacuum pressure (Pa)	87000	101000

Table 1 Material properties of the RI simulations

Experiment	V_f	$\hat{f}_z$(kN)	$\dot{h}_1$(mm/min)	h_1 (mm)	h_2 (mm)	p_{inj} (kPa)	RR (kN/min)
CRTM	0.50	7.5	4.96	4.4011	3.4680	430.1	120

Table 2 Experimental program (RR=Ramp rate, $\hat{f}_z$ is the target force, h_1 is the injection height, h_2 the final height)

$$\begin{cases} \boldsymbol{u} = -\dfrac{1}{\mu}\boldsymbol{K}\nabla p \\ \nabla(h\boldsymbol{u}) = -\dfrac{\partial h}{\partial t} \equiv \dot{h} \end{cases} \quad (1)$$

Here, $\boldsymbol{u}$(x, y, z, t) denotes the volume averaged (or Darcy) velocity, t the time, μ the fluid viscosity, h(x, y, z, t) the mould cavity's thickness, and p(x, y, z, t) is the fluid pressure. The permeability tensor $\boldsymbol{K}$(x, y, z, t) of the reinforcement is a measure of the ability of a fluid to flow through the fabric, and depends mainly on the reinforcement's structure and its fiber volume fraction (V_f).

In the present study, a 3D finite element mesh is used, however, through-thickness flow is neglected [11]. This is reasonable in many practical cases, as the thickness of a composite part is usually orders of magnitude smaller than the other two dimensions. As such, the fluid flow is simulated by solving the Darcy equation (Equations (1)) in 2D. At the flow front a zero pressure boundary condition ($p = 0$) is set. The flow front is tracked by means of fill factors. Every node of the computational grid is assigned a value I that indicates whether the control volume of that node is full (I =1), empty (I =0) or at the flow front (0< I<1).

In the RTM case, the condition $p= p_{inj}$ is set, to drive the fluid through the preform, with p_{inj} the injection pressure. In the CRTM case, a certain $\dot{h}$ is set that is the driving force. For RI, the boundary conditions for the pressure are similar to RTM, where the injection pressure can be approximated as $p_{inj} = p_{atm}$, the atmospheric pressure.

2.2. Elastic reinforcement compaction response models

In this study, two different nonlinear elastic models are used. This is to be able to compare our RI simulation results with the results published in other work. The models essentially describe the thickness of the laminate as a function of the pressure applied to the reinforcement. The equations can be found in the table with the material data, Table 1.

2.3. Viscoelastic reinforcement compaction response model

Kelly et al. proposed a reinforcement compaction model that incorporates viscoelasticity [9,10,12]. It is based on the assumption that different stress-V_f relations, i.e. for different compaction velocities, collapse to a single master function when scaled.

The model deals with compaction and relaxation separately. The first part models the compaction response, and is used when $\dot{h} = 0$. The stress during compaction σ_c, a function of V_f and h, decomposes multiplicatively according to:

$$\sigma_c(V_f, \dot{h}) = \frac{1}{\lambda}\sigma_a(\dot{h})\sigma_b(V_f) \tag{2}$$

with

$$\sigma_b(V_f) = \sum_{i=1}^{N_b} b_i (V_f - {V_f}^{\text{dat}})^i \tag{3}$$

$$\sigma_a(\dot{h}) = \sigma_a(\infty) - [\sigma_a(\infty) - \sigma_a(0)] \frac{1}{N_a} \sum_{i=1}^{N_a} e^{-a_i(\dot{h}/\dot{h}^{\text{ref}})} \tag{4}$$

The function σ_b is the stress (compaction curve), corresponding to the reference compaction speed $\dot{h}^{\text{ref}}$; it is a smooth monotonic curve and can therefore be represented using a simple polynomial function. ${V_f}^{\text{dat}}$ denotes some chosen (small) datum volume fraction corresponding to a measured nominal stress. The second function, σ_a, is the stress at the reference volume fraction ${V_f}^{\text{ref}}$. Due to the rapid initial increase in stress with compaction speed, a polynomial fit is inadequate, however, it is possible to model this behaviour using the formal function Equation (4), where $\sigma_a(\infty)$ and $\sigma_a(0)$ are the stresses at "very fast" and "very slow" speeds, at ${V_f}^{\text{ref}}$, respectively. Finally, it is chosen that $\lambda = \sigma_a(\dot{h}^{\text{ref}}) = \sigma_b({V_f}^{\text{ref}})$. The number of coefficients a_i and b_i to fit the experimental data, N_a and N_b, can be chosen arbitrarily.

The second part of the viscoelastic model concerns the relaxation response, i.e. when $\dot{h} \neq 0$. The relaxation stress can be expressed as a summation of $\sigma_{\text{eq}}(V_f)$, the equilibrium stress, i.e. the

stress at infinitely slow compaction velocity, and q, the viscous stress [11]. In general, q can be determined by solving a differential equation. However, at constant V_f, the differential equation

$$q(t) = [At^n + q_0^{-m}]^{-1/m} \tag{5}$$

can be solved exactly. In Equation (5), $m = (n-1)/n$, $A = nE^{1/n}/\mu$, q_0 is the viscous stress at the start of relaxation, and n, E and μ are material parameters. Incorporating the collapsing behaviour gives

$$\sigma_r(\bar{t}) = \frac{\sigma^R}{\sigma_b(V_f)}\left\{\sigma_{eq}(V_f) + \left[A\left(\bar{t}\frac{\dot{h}^R}{\dot{h}^{ref}}\right)^n + \left(\sigma_b(V_f) - \sigma_{eq}(V_f)\right)^{-m}\right]^{-1/m}\right\} \tag{6}$$

where $\bar{t}$ is the time since the onset of relaxation, σ^R is the stress at the onset of relaxation, $\dot{h}^R$ the compaction speed prior to relaxation, $\sigma_{eq}(V_f)$ can be determined using Equation (2) and the three relaxation parameters are A, m and n. This approach models the collapsing of relaxation curves at a certain V_f. As the relaxation behaviour also depends on V_f one of the parameters must vary with V_f. In this case it is assumed to be A, which can be expressed as a polynomial

$$A(V_f) = \sum_{i=0}^{N_a} A_i {V_f}^i \tag{7}$$

3. Example of a CRTM simulation

To demonstrate the current capabilities of SimLCM and the importance of the viscoelasticity we give an example of a CRTM simulation, and compare the results with experimentally obtained data. The experimental parameters are summarised in Table 3, and the material characterising parameters for the applied glass fibre chopped strand mat (CSM) reinforcement can be found in Table 4. The experiments and the material characterisation is described in more detail in [21,22].

Figures 1 shows the results of the simulation of the CRTM process. The figure displays results as a function of time: the total clamping force, the fibre volume fraction, and the fluid pressure at the inlet. The time axis of the simulation data is shifted so that the start of the second compression phase coincides for the simulation and the experiment. This has been done for ease of comparison during the constant force compression stage. The first stage of the experiment is a dry, velocity controlled compaction, followed by pressure driven injection. This is marked by zero fluid pressure, and a modest increase in force and V_f. Next, the fluid is injected. Here, the force increases due to an increase in fluid pressure, with no change in V_f. This stage is followed by the secondary compression stage. Finally, there is a period of stress relaxation and equilibration.

Property	Dry CSM	Wet CSM	Property	Dry CSM	Wet CSM
Fibre density	2.58 g/cm^3		b_1	76129	79721
Friction coefficient	0.189		b_1	1193200	1249100
$\bar{A}$	3.078e-8		b_1	7890000	7786400
$\bar{B}$	-12.97		b_1	28253000	23959000
Vf^{dat}	0.425		b_1	47027000	30040000
$\dot{h}_{ref}$	2 mm/s		m	0.5	0.5495
$\sigma_a(0)$	30000	30000	n	0.5	0.5331
$\sigma_a(\infty)$	90000	90000	A_1	-0.0233	0.0421
a_1	8000	80	A_2	0.0197	-0.0428
a_2	2.9	1.5	A_3	-0.0036	0.011
a_3	0.8	1.23	K	$K = \bar{A}\exp(\bar{B}\,V_f)$	

Table 3 Material properties for the CRTM process

The first stage of the experiment, i.e. the dry compaction is predicted accurately. The compaction time is predicted accurately as the mould closing velocity is an input parameter. The clamping force, however, is computed with Equation 2, which proves to be a good model. The filling time and the clamping force of the first filling stage, is slightly underestimated in simulation.

The underestimation may be explained by global and spatial variability in reinforcement permeability and compaction response, which is not currently addressed in the simulation. Walbran et al. [22] noted a variation of 10% in fill time between sets of five equivalent experiments, due to stochastic variability of fibre density. Also, a constant permeability value throughout the preform is assumed, which may yield an underestimation of filling time [5]. The agreement between the experimental data and the presented simulations is, however, better than for other (visco-)elastic models. The comparison of the viscoelastic model used here and elastic models, mixed-elastic models and other viscoelastic models is beyond the scope of this paper, but can be found in [21]. The simulated long term relaxation response agrees well with the experimental value.

4. Extension towards the simulation of RI

The essential difference between a (C)RTM and a RI process is the locally changing laminate thickness. The RI process can be seen to be a combination of RTM with imposed injection pressure conditions, and CRTM with changing laminate thickness. However, in the CRTM case, $\dot{h}$ is known before one computes a new pressure distribution. In the RI case, the pressure distribution influences the height profile, and thus the local volume fractions and permeability values. $\dot{h}$ is unknown at each timestep, and therefore an iterative method is necessary.

Given a certain fluid distribution, laminate thickness profile and boundary conditions for the pressure, a new pressure distribution is computed. This new pressure distribution induces the

fluid to flow with a certain velocity that depends on the local permeability. As the fluid flows, however, the preform is wetted and less compressed, the local thickness changes and thus also the permeability.

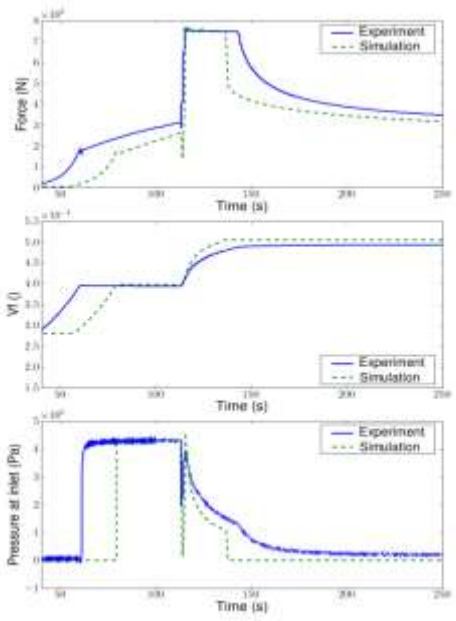

Figure 1. Results of the CRTM simulation and comparison with experimental data

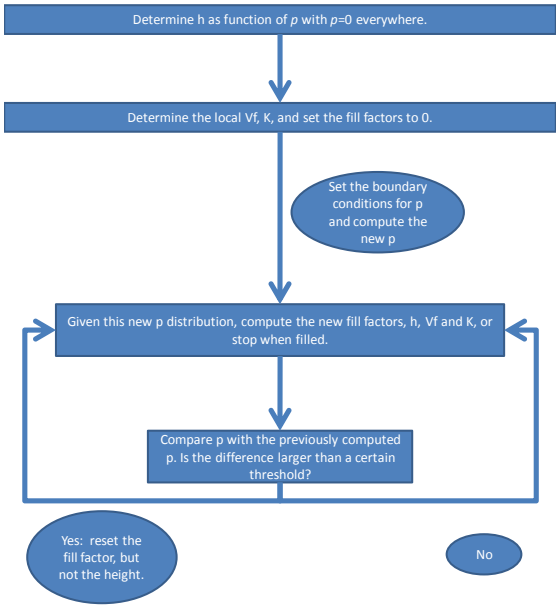

Figure 2. Flowchart demonstrating the iterative process used in the RI solver

The used fluid velocity was thus wrong, as it was based on the old permeability. In the iteration, the fluid flow front is set back to the old value, and the pressure and the velocity are now again computed, but with the new height and permeability profile. This iteration is carried out until the two computed pressure distributions do not differ more than a set value. Then, the next time step is computed, until the mould is filled. This procedure is summarised in the flowchart of Figure 2. To speed up the computational time, the $\dot{h}$ flux term has been neglected in this version of the RI simulation.

5. Comparison with other solvers and experiments

5.1. Comparison with a 1D solver

The University of Auckland LCM research group developed a 1D RI solver which is described in detail in [6,8]. The solver uses a different approach to track the flow front, to that proposed in this paper. Instead of using filling factors, it uses the 'floating node technique'. This technique uses a fixed grid of nodes. Extra nodes are temporarily placed within elements at the flow front, precisely where the flow front sits. This 1D solver does take the $\dot{h}$ flux term into account.

The 1D geometry consits of a 1D flat plate with a length of 0.8 m. The mould is filled with the material as specified in Table 1 [8]. For the 2.5D solver, a similar but 2D geometry is used. The 2D geometry is a flat plate of 0.8x0.4 m^2, filled with the same material. The 1D solver computes a fill time of 1595s, the 2D solver 1618s.

5.2. Comparison with another 2.5 solver and experimental data

Kessels et al. presented a 2.5D RI solver, and experimental validation [13]. In this section we present the comparison of our simulations with their results. The mould in this case is a square flat plate of 0.2x0.2 m^2. The properties of the used material are described in Table 1.

For three instances during the simulation process, Figure 3 presents the computed pressure distribution and the laminate thickness profile. The two subfigures on the left are the situation at the start of the process, the middle two when the mould is half filled, and the two subfigures on the right when the mould is completely filled. Note the typical shape of the laminate thickness profile during RI in the middle of the process: The dry part of the laminate is fully compressed and still at the same thickness as during the initial stage. At the flow front, the laminate is wet, but the fluid pressure at the flow front is still close to zero. Thus, at the flow front the laminate thickness is less than within the dry portion. At the inlet boundary, the fluid pressure has risen in the meanwhile, and the laminate has relaxed to a higher thickness than at the flow front.

Kessels et al. present detailed data on the material they used and the experiments they performed [13]. In Table 1, these data have been summarised. Figure 4 shows a comparison between the results of our simulation, and the simulations and experiments of Kessels et al. Note that the data on the figure is not based on the raw data of Kessels et al. but is approximated by reading directly from the figure in the paper. There is a good agreement between the two simulations, and the results from both simulations are within the experimental data range.

5.3. Discussion

The previous two sections have shown that SimLCM is now capable of basic 2.5D RI simulation. Although the flux originating from $\dot{h}$ is neglected, the results of our simulations agree well with the results from solvers that include that term. The RI results in this paper were obtained using elastic compaction response models. Moreover, other influential parameters such as variability are not included in this study. Still, the comparison with experimental data shows that with this simplified compaction model, good predictions for the filling phase can be obtained.

6. Conclusion and further research

A generic LCM filling simulation is under development at the University of Auckland, SimLCM. This paper describes the extension of SimLCM to the simulation of RI. This paper presented the first step towards an accurate and complete RI solver. The results of the simulations were compared with the results of other solvers and experimental data and show good agreement.

Future research will concern the inclusion of reinforcement viscoelasticity and permanent deformation into the simulation. Although elastic models give good results for the simulation of the filling process, these effects play an important role in the post-filling stage of LCM-processes. Besides more complex reinforcement compaction behaviour and the accurate simulation of the pre and post-filling stages, the effects of reinforcement variability will also be included inot the SimLCM software.

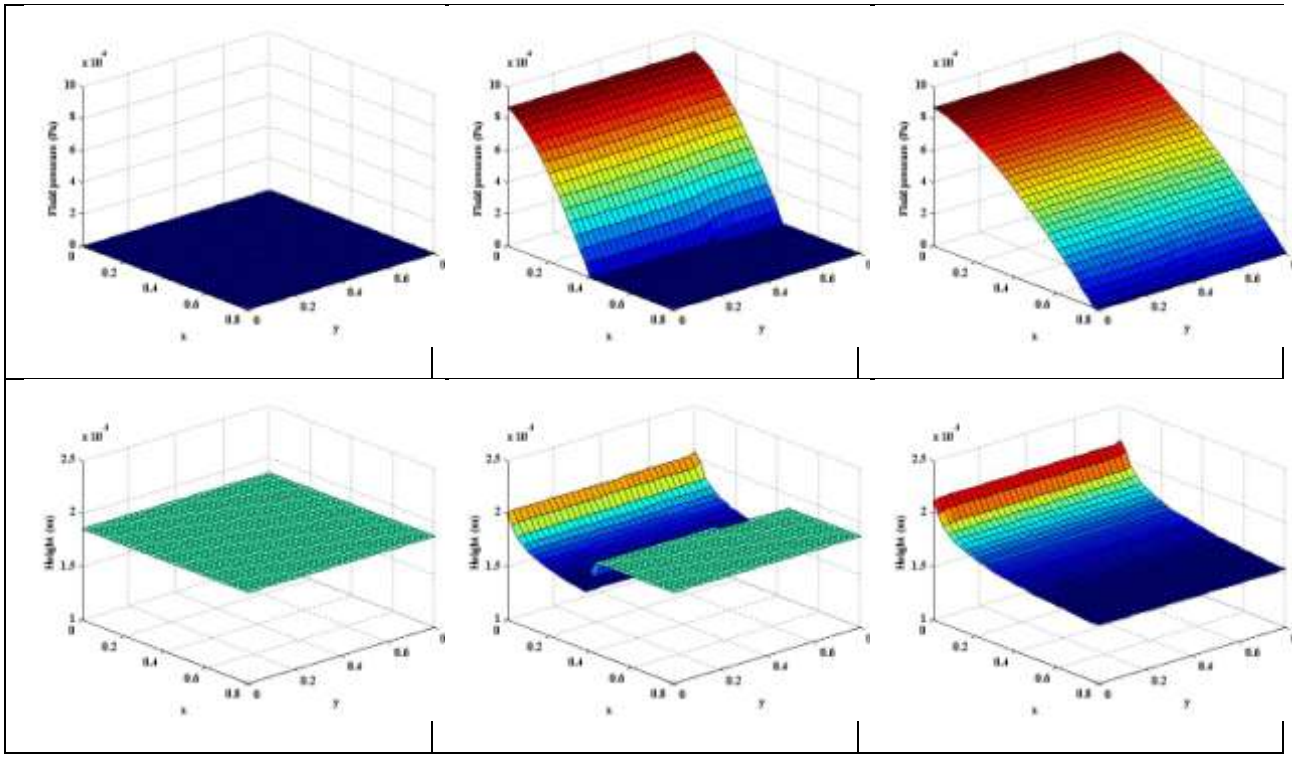

Figure 3. Visualization of the results of the 2.5D RI simulation: (left) at the start of the process, (middle) half way through the process, (right) when the mould is completely filled

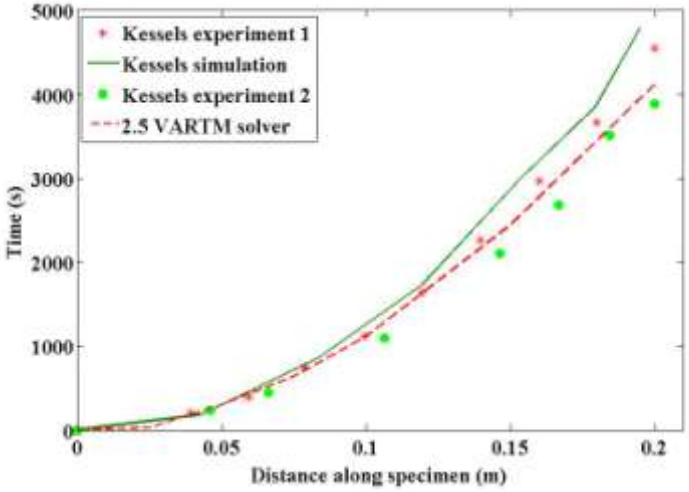

Figure 4. Comparison of the experimental and simulation data of Kessles et al. [13] and our 2.5D RI solver

7. References

[1] Bickerton, S. and Abdullah, M.Z.: "Modeling and evaluation of the filling stage of injection/compression moulding" *Composites Science and Technology*, 63(10), 2003.
[2] Chang, C.Y.: "Simulation of mold filling in simultaneous resin injection compression molding" *Journal of Reinforced Plastics and Composites*, 25 (12):1255-68, 2006.
[3] Chen, S.C., Chen, Y.C., and Cheng, N.T.: "Simulation of injection compression mold filling process" *International Communications in Heat and Mass Transfer*, 25(7):907-17, 1998.
[4] Deleglise, M., Binetruy, C. and Krawczak P.: "Simulation of lcm processes involving induced or forced deformations" *Composites Part A: Applied science and manufacturing*, 37(6):874-80, 2006.
[5] Endruweit, A., Long, A.C., Robitaille, F. and Rudd, C.D.: "Influence of stochastic fibre angle variations on the permeability of bi-directional textile fabrics" *Composites Part A: Applied science and manufacturing*, 37:122132, 2006.
[6] Govignon, Q., Bickerton, S., Kelly, P.A.: "Simulation of the reinforcement compaction and resin flow during the complete resin infusion process", *Composites Part A: Applied science and manufacturing*, 41:45-57, 2010.
[7] Han, K., Toth, J., Lee, L.J. and Green, J.P.: "Analysis of an injection/compression liquid composite molding process" *Polymer Composites*, 19(4): 487-96, 1998.
[8] Johnson, C.: "Modelling of composite materials manufacturing processes", Part IV project, Department of Engineering Science, The University of Auckland.
[9] Kelly, P.A.: "A fibre compaction model for liquid composite moulding" *Proceedings of the 6th Canadian International composites conference (CANCOM)*, August 2007.
[10] Kelly, P.A.: A viscoelastic model for the compaction of fibrous materials. *Journal of the Textile Institute*, 2010. Submitted.
[11] Kelly, P.A. and Bickerton, S.: "A comprehensive filling and tooling force analysis for rigid mould LCM processes" *Composites Part A: Applied science and manufacturing*, 2009. doi: 10.1016/j.compositesa.2009.07.013.
[12] Kelly, P.A., Umer, R. and Bickerton, S.: "Viscoelastic response of dry and wet fibrous materials during infusion processes" *Composites Part A: Applied science and manufacturing*, 6:868-873, 2006.

[13] Kessels, J.F.A, Jonker, A.S. and Akkerman R.: "Fully 2.5D flow modelling of resin infusion under flexible tooling using unstructured meshes and wet and dry compaction properties" *Composites Part A: Applied science and manufacturing*, 38:51-60, 2007
[14] Lin, R.J. and Liou, M.J.: "Mold filling and curing analysis liquid composite molding" *Polymer Composites*, 14(1):7181, 1993.
[15] Mohan, R.V., Ngo, N.D.: and Tamma, K.K. "On a pure finite-element-based methodology for resin transfer mold filling simulations" *Polymer Engineering Science*, 39(1):2643, 1993.
[16] Pham, X-T and Trochu, F.: "Simulation of compression resin transfer molding to manufacture thin composite shells" *Polymer Composites*, 20(3):436-59, 1999.
[17] Shojaei, A.: "Numerical simulation of three-dimensional flow and analysis of filling process in compression resin transfer moulding" *Composites Part A: Applied science and manufacturing*, 37(9):1434-50, 2006.
[18] Simacek, P. and Advani, S.G.: "Desirable features in mold filling simulations for liquid composite molding processes" *Polymer composites*, 25(4):355-367, 2004.
[19] Trochu, F., Gauvin, R. and Gao, D.M.: "Numerical analysis of the resin transfer molding process by the finite element method" *Advances in Polymer Technology*, 12(4):329-42, 1993.
[20] Trochu, F. Ruiz, E., Achim, V. and Soukane, S.: "Advanced numerical simulation of liquid composite molding for process analysis and optimization" *Composites Part A: Applied science and manufacturing*, 37(6):890-902, 2006.
[21] Walbran, W.A., Verleye, B., Bickerton, S. and Kelly, P.A.: "Reducing setup costs: Tooling force prediction in resin transfer moulding (RTM) and compression RTM" *Proceedings of the 9th annual Automotive Composites Conference and Exhibition (ACCE09)*, pages 1-18. Society of Plastics Engineers, Automotive and Composites Divisions, September 2009. URL http: //www.speautomotive.com/SPEA_CD/SPEA2009/pdf/ET/ET-08.pdf.
[22] Walbran, W.A., Bickerton, S. and Kelly, P.A.: "Measurements of normal stress distribution experienced by rigid liquid composite moulding tools" *Composites Part A: Applied science and manufacturing*, 40:1119-1133, 2009. doi: 10.1016/j.compositesa.2009.05.004